Checkpoint Inhibitor Immunotherapy to Treat Temozolomide-Associated Hypermutation in Advanced Atypical Carcinoid Tumor of the Lung

Fangdi Sun, MD[1]; James P. Grenert, MD, PhD[2]; Lisa Tan, BS[1]; Jessica Van Ziffle, PhD[2]; Nancy M. Joseph, MD, PhD[2]; Claire K. Mulvey, MD[1]; and Emily Bergsland, MD[1]

JCO Precis Oncol 6:e2200009. © 2022 by American Society of Clinical Oncology

Introduction

Pulmonary neuroendocrine tumors (NETs) have a wide spectrum of clinical behaviors, ranging from indolent well-differentiated (WD) NETs (typical carcinoids) to aggressive, poorly differentiated neuroendocrine carcinomas (NECs) including large cell NEC and small-cell lung cancer (SCLC).[1] Atypical carcinoids are an uncommon type of WD NET with an intermediate grade and prognosis. Compared with typical carcinoids, these tumors are more commonly nonfunctional and somatostatin receptor–negative and have worse prognosis.[2]

Therapy for advanced pulmonary carcinoids remains ill-defined, extrapolated from WD gastroenteropancreatic NETs and poorly differentiated lung NECs. Few prospective studies have included these neoplasms, and even the role of somatostatin analogs is uncertain. Everolimus was approved on the basis of a phase III trial not powered for the lung subgroup; practically, its use is restricted to patients with relatively indolent disease.[3,4] The angiogenesis inhibitor surufatinib has activity in nonpancreatic NETs; however, lung NETs accounted for only 11.6% of patients in the pivotal trial.[5] Although approved in SCLC, the role of immunotherapy in unselected WD lung NETs remains ill-defined.[6-11] Data from small retrospective series suggest that platinum-etoposide, temozolomide (TMZ) monotherapy, and TMZ/capecitabine regimens have clinical activity in advanced pulmonary carcinoids.[12-14]

TMZ is an oral alkylating prodrug that methylates DNA at O^6 guanine residues (O^6-meG), causing mismatch pairing during DNA replication, leading to genomic instability, apoptosis, and cell death. TMZ cytotoxicity depends on an intact DNA mismatch repair (MMR) pathway and low levels of O^6-methylguanine DNA methyltransferase (MGMT).[15-17] MGMT-mediated repair is stoichiometrically limited, and in malignant gliomas and melanoma, MGMT deficiency is associated with TMZ response.[18-23] This relationship is less clear in NETs.[24-26] The absence of MGMT-mediated repair coupled with defective MMR (dMMR) leads to enrichment of C:G>A:T transitions throughout the genome, a marked increase in tumor mutational burden (TMB), and loss of TMZ-induced cytotoxicity, a resistance mechanism termed TMZ-associated hypermutation.[27-33]

TMZ-associated hypermutation is well-demonstrated in malignant glioma and is frequently associated with inactivating alterations in DNA MMR genes.[34] The use of immunotherapy for TMZ-associated hypermutation falls under tumor-agnostic approvals of pembrolizumab for high TMB, microsatellite instability (MSI)-high, or dMMR solid tumors. There are few reports of TMZ-associated hypermutation in NETs, and none to our knowledge in atypical lung carcinoids.[35] Here, we describe a patient with treatment-refractory atypical carcinoid tumor of the lung who developed TMZ-associated hypermutation that responded to checkpoint inhibitor immunotherapy.

Patient Consent Statement

Approval for the release of health information was obtained from the patient referenced in this report as requested by *JCO Precision Oncology* editorial.

Case Presentation

A 66-year-old man presented with right-sided chest pain. Computed tomography (CT) scan demonstrated a 3.8-cm right lung mass, mediastinal and hilar lymphadenopathy, and multiple hepatic masses up to 4.5 cm. Liver biopsy showed WD NET with immunohistochemistry (IHC) positive for synaptophysin, chromogranin, and thyroid transcription factor-1 (3 mitoses per 2 mm^2, Ki-67 14.4%; Fig 1, biopsy 1), consistent with metastatic atypical carcinoid tumor. Next-generation sequencing (NGS) of the liver metastasis (UCSF 500 Cancer Gene Panel [UCSF500], done retrospectively for research analysis) showed no pathogenic variants, a single variant of uncertain significance in *EED*, TMB 5.5 mutations/megabase (Mb), and no unstable microsatellites by MSIsensor (Table 1, t = 0).[42] ^{68}Ga-DOTATATE scan revealed uptake in the lung mass but not the hepatic lesions, which demonstrated relatively high fluorodeoxyglucose avidity on ^{18}F-labeled

ASSOCIATED CONTENT

Appendix

Author affiliations and support information (if applicable) appear at the end of this article.

Accepted on May 4, 2022 and published at ascopubs.org/journal/po on June 23, 2022: DOI https://doi.org/10.1200/PO.22.00009

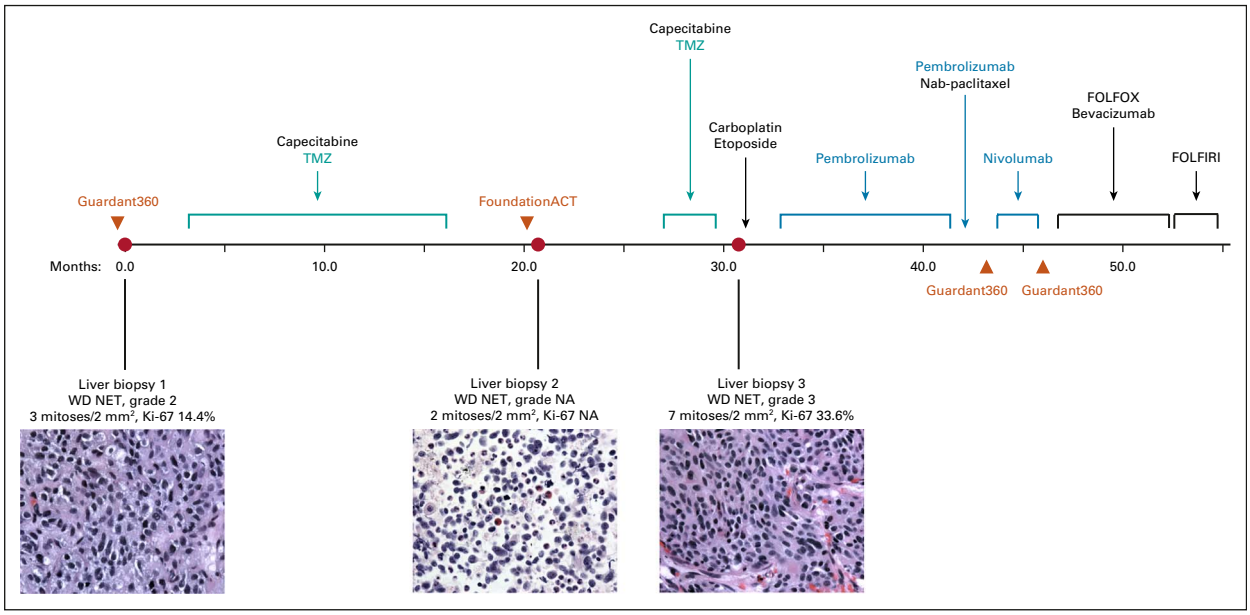

FIG 1. Chronological timeline of diagnostic liver biopsies (red circles), plasma ctDNA assessments (orange triangles), and treatment course of an atypical carcinoid tumor of the lung with TMZ-associated hypermutation treated with checkpoint inhibitor immunotherapy. Included is hematoxylin and eosin staining of histopathologic liver biopsy specimens at 60× magnification. ctDNA, circulating tumor DNA; FOLFIRI, fluorouracil, leucovorin, and irinotecan; FOLFOX, infusional fluorouracil, leucovorin, and oxaliplatin; NA, not available; NET, neuroendocrine tumor; TMZ, temozolomide; WD, well-differentiated.

fluorodeoxyglucose positron emission tomography (standardized uptake value 13.2).

The patient received 14 cycles of TMZ/capecitabine with partial response in the lung and stable disease in the liver and retroperitoneal lymph nodes. The lung mass and thoracic lymphadenopathy were stable throughout the remaining clinical course. When a later CT scan showed a new 0.8 cm hepatic hypodensity, he underwent a second liver biopsy that revealed a WD NET (2 mitoses per 2 mm^2, Ki-67 not available), with NGS (UCSF500, done retrospectively for research analysis) demonstrating the same variant of uncertain significance, $<$ 10 somatic mutations, and a frameshift mutation in *MLH1*. TMB was 13.1 mutations/Mb, with 15% unstable microsatellites (Fig 1, biopsy 2; Table 1, t = 21.0 months). He subsequently developed rapidly progressive liver metastases and retroperitoneal lymphadenopathy, for which he received three additional cycles of TMZ/capecitabine without benefit. A third liver biopsy again demonstrated thyroid transcription factor-1(+) WD NET (7 mitoses per 2 mm^2), and the patient received three cycles of carboplatin/etoposide without benefit (Fig 2B). NGS (UCSF500) revealed $>$ 80 somatic mutations, including two splice site mutations in *MLH1* not present in the germline sample, consistent with a hypermutator phenotype from acquired dMMR (Table 1, t = 31.1 months; Appendix Table A1). Notably, nearly all the somatic mutations were C:G>T:A mutations. TMB had increased to 89.6 mutations/Mb with 14% unstable sites. Pathology review confirmed WD NET (Ki-67 33.6%), with the absence of MLH1 and PMS2 protein expression by IHC (Fig 1, biopsy 3).

The patient was treated with pembrolizumab (200 mg intravenously once every 3 weeks) for 9 months, with a marked interval decrease in the hepatic metastases and retroperitoneal lymphadenopathy after cycles 4 and 7 (Fig 2C). Magnetic resonance imaging after cycle 12 showed worsening hepatic and new osseous metastases (Fig 2D), for which nab-paclitaxel was added (three cycles). Faced with ongoing multifocal progression, the patient was switched to ipilimumab/nivolumab for 2 months without success.[11] He was then treated with modified infusional fluorouracil, leucovorin, and oxaliplatin-6 plus bevacizumab for 6 months. After progressing on an irinotecan-based regimen, the patient succumbed to his disease almost five years after initial diagnosis.

Discussion

Emerging data support the use of TMZ-based therapy in NETs, with TMZ/capecitabine demonstrating superiority to single-agent TMZ in pancreatic tumors.[43-45] There are few reports of TMZ-associated hypermutation beyond malignant glioma: two in pancreatic NETs, one in high-grade cervical NET, and one in pituitary carcinoma.[35,46,47] For this patient, NGS identified two *MLH1* splice site mutations absent in the treatment-naïve liver metastasis. IHC confirmed MLH1 loss in the hypermutated liver metastasis and loss of PMS2, the latter likely because of degradation of the undimerized partner of MLH1.[48] There were no findings on germline analysis to explain the pattern of somatic

TABLE 1. Summary of Serial Molecular Profiling Performed on Both Tissue and Plasma Specimens Throughout the Clinical Course, Specifically Pathogenic or Likely Pathogenic Alterations, as Defined by Each Proprietary Testing Platform

		Same Tissue Specimen			Same Tissue Specimen				
Time	**t = –0.2 Months**	**t = 0 (tissue diagnosis)**		**t = 20.3 Months**	**t = 21.0 Months**		**t =31.1 Months**	**t = 43.2 Months**	**t = 46.0 Months**
Source	Plasma	**Tissue (liver)**	Tissue (liver)	Plasma	**Tissue (liver)**	Tissue (liver)	**Tissue (liver)**	Plasma	Plasma
Specific test	Guardant360[36]	**UCSF500[37,a]**	STAMP[38]	FoundationACT[39]	**UCSF500[37,a]**	GPS Cancer (NantHealth)[40]	**UCSF500[37]**	Guardant360[36]	Guardant360[36]
No. of genes assessed	70	**529**	130	62	**529**	Whole-genome DNA sequencing	**479**	74	74
Normal tissue for comparison	No	**Yes**	No	No	**Yes**	Yes	**Yes**	No	No
MSI status	NR	**MSS**	NR	NA	**MSS**	MSS	**MSS**	MSI-H	MSI-H
TMB (mutations/Mb)		**5.5**			**13.1**	7.3	**89.6**		
Unstable microsatellites (%)		**0**			**15.29**	8.02	**14.05**		
No. of somatic alterations		**1**			**5**	—	**86**		
Pathogenic or likely pathogenic alterations[b] (allele frequency or copy number; OncoKB therapeutic level[41,c])	None	**None**	None	AKT1 p.E17K (0.16%; level 3A—breast, endometrial, and ovarian cancer) KRAS p.G12D (0.16%; level 4—all solid tumors) NF1 p.P1222fs*2 (0.52%; level 4—all solid tumors) ALK p.T1102I (0.17%) TP53 p.G244D (0.38%) TP53 p.R273H (0.23%) TP53 p.K382fs*40 (0.17%) TP53 p.L130F (0.15%)	**MLH1 p.M342fs (52%)**	None	**MLH1 p.M342fs (44%)** **MLH1 c.208-1G>A (59%)** **TP53 p.G244D (34%)**	STK11 splice site SNV (0.4%, level 4—all solid tumors) CCND2 amplification (plasma copy number 2.8) EGFR p.G796D (0.6%) EGFR p.R1052K (0.3%) MYC p.P75S (0.3%) TP53 p.G244D (33.6%) TP53 p.A138V (0.3%) TP53 splice site SNV (0.3%) TP53 p.G108D (0.2%) TP53 p.T253A (0.1%)	EGFR p.G796D (0.3%) TP53 p.G244D (42.1%) TP53 p.R273C (0.2%) TP53 p.P151S (0.1%)

NOTE. Bold entries are tissue specimens analyzed across the same sequencing platform, UCSF500, demonstrating acquisition of two splice site mutations in *MLH1* and a significant increase in TMB.

Abbreviations: Mb, megabase; MSI, microsatellite instability; MSI-H, microsatellite instability-high; MSS, microsatellite stable; NA, not available in abbreviated report; NR, not reported by testing platform; TMB, tumor mutational burden.

[a]Indicates results that were collected as part of research analysis, which were not available at the time of clinical decision making.

[b]Defined individually by each proprietary sequencing platform.

[c]If no level is indicated in parentheses, no therapeutic level is annotated by OncoKB for the specific alteration listed.

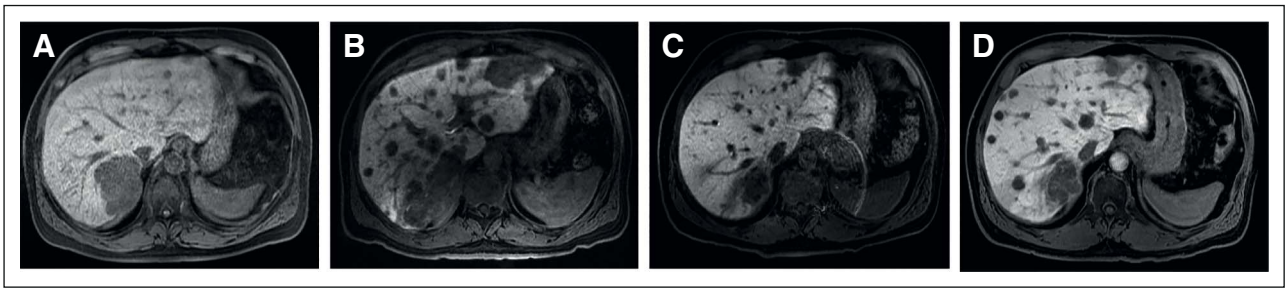

FIG 2. MRI of the abdomen/pelvis (T2-weighted, postgadolinium, LAVA) demonstrating progression of hepatic metastases on TMZ followed by partial response to pembrolizumab immunotherapy. Representative images (A) during treatment holiday before the last three cycles of TMZ/capecitabine (maximum lesion diameter: 7.3 cm); (B) after three cycles of carboplatin/etoposide, before initiation of pembrolizumab (maximum lesion diameter: 9.0 cm); (C) after eight cycles of pembrolizumab (maximum lesion diameter: 4.4 cm); and (D) after 12 cycles (9 months) of pembrolizumab (maximum lesion diameter: 7.0 cm). LAVA, liver acquisition volume acceleration; MRI, magnetic resonance imaging; TMZ, temozolomide.

hypermutation. Although MSI is a clinical biomarker for dMMR, it is defined on the basis of data from colorectal and endometrial carcinomas, and it remains unclear whether these traditional cutoffs apply to other tumor types. Technically, this dMMR lung NET was microsatellite stable. However, it has been shown that dMMR gliomas deemed microsatellite stable might actually have a MSI phenotype better characterized by single-cell whole-genome sequencing than standard NGS panels.[49,50] This case demonstrated an increase from 0% unstable microsatellites in the first biopsy to 15% and 14% unstable microsatellites in the second and third biopsies, respectively. Taken together, these data suggest that TMZ-associated hypermutation occurs in NETs as a mechanism of resistance, and some, but not all, of the increased TMB is a result of increased MSI.

Few immunotherapy trials have enrolled pulmonary NETs other than SCLC, and none has explored immunotherapy for hypermutated tumors.[11,51-54] Although results have generally been disappointing, a 17% overall response rate was observed for spartalizumab in bronchial NETs.[6-8] Limited data suggest that combination therapy (eg, ipilimumab/nivolumab) may be more active, but additional information about the relationship between response and molecular markers (eg, TMB and MSI status) is needed. In gliomas, response to immunotherapy has been observed in a subset of dMMR gliomas, but overall response rate to programmed death-1 blockade was low in a series of 11 patients.[50,55] At least two potential mechanisms underlie this observation. In contrast to colorectal cancer, dMMR gliomas lack significant T-cell infiltrates, despite a similar nonsynonymous mutational burden.[50] Furthermore, hypermutation in gliomas with acquired dMMR tends to be subclonal and does not generate optimal antitumor T-cell responses. The use of immunotherapy for NETs with TMZ-associated hypermutation has only been reported in one other case (high-grade cervical NET).[46] There, a subclonal MSH6 nonsense mutation was identified, but MMR deficiency was not confirmed with MSH6 loss by IHC or MSI testing.

In this case, serial tissue biopsy with concomitant NGS identified increasingly aggressive features (mitotic rate and proliferation index) and genomic evolution after treatment, most evident when analyzed retrospectively with a single platform (UCSF500) and akin to previous studies of pancreatic NETs.[35] This patient had additional tissue and plasma NGS ordered in real time at various time points by different providers (Table 1), but the clinical utility of such testing was limited given significant heterogeneity between testing platforms (eg, limits of detection, number of genes assessed, and use of normal control) and lack of disease-specific guidance in this area.

In this case, the identification of a hypermutated phenotype with dMMR and high TMB prompted subsequent treatment with immunotherapy, which led to partial response and disease control for 9 months. Although the role of repeat tissue biopsy and molecular profiling in atypical bronchial carcinoid remains ill-defined, this case suggests that it is worth considering in patients treated with TMZ given the potential for identifying mutational signatures that could guide therapy. Additional studies are required to delineate the optimal strategy for molecular profiling, in both tissue and plasma. Furthermore, the association between the hypermutated phenotype and response to immunotherapy is not definitive in this case. Such a link could be further explored in a prospective study or at least a larger retrospective cohort (recognizing the response rate in biomarker-unselected bronchial NETs is low).[6,7,9-11] Although the incidence of TMZ-associated hypermutation in NETs is unknown, its presence should alert clinicians to the potential value of immunotherapy, recognizing that the precise relationship between TMZ-associated hypermutation, dMMR, immune microenvironment, and response to immunotherapy requires further study.

AFFILIATIONS

[1]Division of Hematology and Oncology, Department of Medicine, University of California, San Francisco, San Francisco, CA
[2]Department of Pathology, University of California, San Francisco, San Francisco, CA

CORRESPONDING AUTHOR

Fangdi Sun, MD, 505 Parnassus Ave, Room M-1483, San Francisco, CA 94143; e-mail: fangdi.sun@ucsf.edu.

DISCLAIMER

The content is solely the responsibility of the authors and does not necessarily represent the official views of the National Institutes of Health.

SUPPORT

Supported by the National Cancer Institute of the National Institutes of Health under award No. P30CA082103.

AUTHOR CONTRIBUTIONS

Conception and design: Fangdi Sun, Emily Bergsland
Collection and assembly of data: Fangdi Sun, Lisa Tan, Jessica Van Ziffle
Data analysis and interpretation: Fangdi Sun, James P. Grenert, Nancy M. Joseph, Claire K. Mulvey, Emily Bergsland
Manuscript writing: All authors
Final approval of manuscript: All authors
Accountable for all aspects of the work: All authors

AUTHORS' DISCLOSURES OF POTENTIAL CONFLICTS OF INTEREST

The following represents disclosure information provided by authors of this manuscript. All relationships are considered compensated unless otherwise noted. Relationships are self-held unless noted. I = Immediate Family Member, Inst = My Institution. Relationships may not relate to the subject matter of this manuscript. For more information about ASCO's conflict of interest policy, please refer to www.asco.org/rwc or ascopubs.org/po/author-center.

Open Payments is a public database containing information reported by companies about payments made to US-licensed physicians (Open Payments).

Jessica Van Ziffle
Employment: Adaptive Biotechnologies (I)
Stock and Other Ownership Interests: Adaptive Biotechnologies (I)
Patents, Royalties, Other Intellectual Property: Adaptive Biotechnologies (I)

Claire K. Mulvey
Honoraria: OncLive/MJH Life Sciences
Research Funding: Genentech

Emily Bergsland
Stock and Other Ownership Interests: More Health (I), Exai Bio (I)
Consulting or Advisory Role: More Health (I)
Research Funding: Merck
Patents, Royalties, Other Intellectual Property: UpToDate

No other potential conflicts of interest were reported.

REFERENCES

1. Travis WD, Rush W, Flieder DB, et al: Survival analysis of 200 pulmonary neuroendocrine tumors with clarification of criteria for atypical carcinoid and its separation from typical carcinoid. Am J Surg Pathol 22:934-944, 1998
2. García-Yuste M, Matilla JM, Cueto A, et al: Typical and atypical carcinoid tumours: Analysis of the experience of the Spanish Multi-centric Study of Neuroendocrine Tumours of the Lung. Eur J Cardiothoracic Surg 31:192-197, 2007
3. Yao JC, Fazio N, Singh S, et al: Everolimus for the treatment of advanced, non-functional neuroendocrine tumours of the lung or gastrointestinal tract (RADIANT-4): A randomised, placebo-controlled, phase 3 study. Lancet 387:968-977, 2016
4. Fazio N, Buzzoni R, Delle Fave G, et al: Everolimus in advanced, progressive, well-differentiated, non-functional neuroendocrine tumors: RADIANT-4 lung subgroup analysis. Cancer Sci 109:174-181, 2018
5. Xu J, Shen L, Zhou Z, et al: Surufatinib in advanced extrapancreatic neuroendocrine tumours (SANET-ep): A randomised, double-blind, placebo-controlled, phase 3 study. Lancet Oncol 21:1500-1512, 2020
6. Strosberg J, Mizuno N, Doi T, et al: Efficacy and safety of pembrolizumab in previously treated advanced neuroendocrine tumors: Results from the phase II KEYNOTE-158 study. Clin Cancer Res 26:2124-2130, 2020
7. Yao J, Strosberg J, Fazio N, et al: Spartalizumab in metastatic, well/poorly-differentiated neuroendocrine neoplasms. Endocr Relat Cancer 28:161-172, 2021
8. Mehnert JM, Bergsland E, O'Neil BH, et al: Pembrolizumab for the treatment of programmed death-ligand 1-positive advanced carcinoid or pancreatic neuroendocrine tumors: Results from the KEYNOTE-028 study. Cancer 126:3021-3030, 2020
9. Klein O, Kee D, Markman B, et al: Immunotherapy of ipilimumab and nivolumab in patients with advanced neuroendocrine tumors: A subgroup analysis of the CA209-538 clinical trial for rare cancers. Clin Cancer Res 26:4454-4459, 2020
10. Capdevila J, Teule A, López C, et al: A multi-cohort phase II study of durvalumab plus tremelimumab for the treatment of patients (pts) with advanced neuroendocrine neoplasms (NENs) of gastroenteropancreatic or lung origin: The DUNE trial (GETNE 1601). Ann Oncol 31:S770-S771, 2020
11. Patel SP, Othus M, Chae YK, et al: A phase II basket trial of dual anti-CTLA-4 and anti-PD-1 blockade in rare tumors (DART SWOG 1609) in patients with nonpancreatic neuroendocrine tumors. Clin Cancer Res 26:2290-2296, 2020
12. Shah MH, Goldner WS, Halfdanarson TR, et al: Neuroendocrine and adrenal tumors, version 2.2018 featured updates to the NCCN guidelines. J Natl Compr Cancer Netw 16:693-702, 2018
13. Chong CR, Wirth LJ, Nishino M, et al: Chemotherapy for locally advanced and metastatic pulmonary carcinoid tumors. Lung Cancer 86:241-246, 2014
14. Wirth LJ, Carter MR, Jänne PA, et al: Outcome of patients with pulmonary carcinoid tumors receiving chemotherapy or chemoradiotherapy. Lung Cancer 44:213-220, 2004
15. Daniel P, Sabri S, Chaddad A, et al: Temozolomide induced hypermutation in glioma: Evolutionary mechanisms and therapeutic opportunities. Front Oncol 9:41, 2019
16. Karran P, Marinus MG: Mismatch correction at O^6-methylguanine residues in *E. coli* DNA. Nature 296:868-869, 1982
17. Margison GP, Santibáñez Koref MF, Povey AC: Mechanisms of carcinogenicity/chemotherapy by O^6-methylguanine. Mutagenesis 17:483-487, 2002
18. Kulke MH, Hornick JL, Frauenhoffer C, et al: O^6-methylguanine DNA methyltransferase deficiency and response to temozolomide-based therapy in patients with neuroendocrine tumors. Clin Cancer Res 15:338-345, 2009
19. Hegi ME, Diserens AC, Gorlia T, et al.: MGMT gene silencing and benefit from temozolomide in glioblastoma. N Engl J Med 352:997-1003, 2005

20. Brandes AA, Tosoni A, Cavallo G, et al: Correlations between O^6-methylguanine DNA methyltransferase promoter methylation status, 1p and 19q deletions, and response to temozolomide in anaplastic and recurrent oligodendroglioma: A prospective GICNO study. J Clin Oncol 24:4746-4753, 2006
21. Chinot OL, Barrié M, Fuentes S, et al: Correlation between O^6-methylguanine-DNA methyltransferase and survival in inoperable newly diagnosed glioblastoma patients treated with neoadjuvant temozolomide. J Clin Oncol 25:1470-1475, 2007
22. Middleton MR, Lunn JM, Morris C, et al: O^6-methylguanine-DNA methyltransferase in pretreatment tumour biopsies as a predictor of response to temozolomide in melanoma. Br J Cancer 78:1199-1202, 1998
23. Esteller M, Garcia-Foncillas J, Andion E, et al: Inactivation of the DNA-repair gene MGMT and the clinical response of gliomas to alkylating agents. N Engl J Med 343:1350-1354, 2000
24. Cros J, Hentic O, Rebours V, et al: MGMT expression predicts response to temozolomide in pancreatic neuroendocrine tumors. Endocr Relat Cancer 23:625-633, 2016
25. Krug S, Boch M, Rexin P, et al: Impact of therapy sequence with alkylating agents and MGMT status in patients with advanced neuroendocrine tumors. Anticancer Res 37:2491-2500, 2017
26. Cives M, Ghayouri M, Morse B, et al Analysis of potential response predictors to capecitabine/temozolomide in metastatic pancreatic neuroendocrine tumors. Endocr Relat Cancer 23:759-767, 2016
27. Yip S, Miao J, Cahill DP, et al: MSH6 mutations arise in glioblastomas during temozolomide therapy and mediate temozolomide resistance. Clin Cancer Res 15:4622-4629, 2009
28. Marra G, D'Atri S, Corti C, et al: Tolerance of human $MSH2^{+/-}$ lymphoblastoid cells to the methylating agent temozolomide. Proc Natl Acad Sci USA 98:7164-7169, 2001
29. Fink D, Aebi S, Howell SB: The role of DNA mismatch repair in drug resistance. Clin Cancer Res 4:1-6, 1998
30. Felsberg J, Thon N, Eigenbrod S, et al: Promoter methylation and expression of MGMT and the DNA mismatch repair genes MLH1, MSH2, MSH6 and PMS2 in paired primary and recurrent glioblastomas. Int J Cancer 129:659-670, 2011
31. Johnson BE, Mazor T, Hong C, et al: Mutational analysis reveals the origin and therapy-driven evolution of recurrent glioma. Science 343:189-193, 2014
32. Cahill DP, Levine KK, Betensky RA, et al: Loss of the mismatch repair protein MSH6 in human glioblastomas is associated with tumor progression during temozolomide treatment. Clin Cancer Res 13:2038-2045, 2007
33. Choi S, Yu Y, Grimmer MR, et al: Temozolomide-associated hypermutation in gliomas. Neuro Oncol 20:1300-1309, 2018
34. Wang J, Cazzato E, Ladewig E, et al: Clonal evolution of glioblastoma under therapy. Nat Genet 48:768-776, 2016
35. Raj N, Shah R, Stadler Z, et al: Real-time genomic characterization of metastatic pancreatic neuroendocrine tumors has prognostic implications and identifies potential germline actionability. JCO Precis Oncol 2018:1-18, 2018
36. Guardant Health: Guardant360® CDx. https://guardant360cdx.com/
37. UCSF Health Center for Clinical Genetics and Genomics: UCSF 500 Cancer Gene Panel Test (UCSF500/UC500). https://genomics.ucsf.edu/content/ucsf-500-cancer-gene-panel-test-ucsf500-uc500
38. Stanford Health Care: Molecular Genetic Pathology—Stanford Tumor Actionable Mutation Pattern for Solid Tumors (STAMP). https://stanfordlab.com/content/stanfordlab/en/molecular-pathology/molecular-genetic-pathology.html/
39. Foundation Medicine: Foundation Medicine Introduces FoundationOne®Liquid, the Latest Advance in the Company's Liquid Biopsy Test for Solid Tumors in Patients With Advanced Cancer (FoundationACT™, Assay for Circulating Tumor DNA, Has Since Been Superceded by FoundationOne® Liquid CDx), 2018. https://www.foundationmedicine.com/press-releases/d67a6b76-e9a9-4f5f-9a0a-c47831980163
40. NantOmics: GPS Cancer™. https://nantomics.com/gpscancer/
41. Chakravarty D, Gao J, Phillips SM, et al: OncoKB: A precision oncology knowledge base. JCO Precis Oncol 1:PO.17.00011, 2017
42. Niu B, Ye K, Zhang Q, et al: MSIsensor: Microsatellite instability detection using paired tumor-normal sequence data. Bioinformatics 30:1015-1016, 2014
43. Al-Toubah T, Morse B, Strosberg J: Capecitabine and temozolomide in advanced lung neuroendocrine neoplasms. Oncologist 25:e48-e52, 2020
44. Koumarianou A, Kaltsas G, Kulke MH, et al: Temozolomide in advanced neuroendocrine neoplasms: Pharmacological and clinical aspects. Neuroendocrinology 101:274-288, 2015
45. Kunz PL, Catalano PJ, Nimeiri H, et al: A randomized study of temozolomide or temozolomide and capecitabine in patients with advanced pancreatic neuroendocrine tumors: A trial of the ECOG-ACRIN Cancer Research Group (E2211). J Clin Oncol 36, 2018 (suppl 15; abstr 4004)
46. Klempner SJ, Hendifar A, Waters KM, et al: Exploiting temozolomide-induced hypermutation with pembrolizumab in a refractory high-grade neuroendocrine neoplasm: A proof-of-concept case. JCO Precis Oncol 4:614-619, 2020
47. Lin AL, Jonsson P, Tabar V, et al: Marked response of a hypermutated ACTH-secreting pituitary carcinoma to ipilimumab and nivolumab. J Clin Endocrinol Metab 103:3925-3930, 2018
48. Chen W, Frankel WL: A practical guide to biomarkers for the evaluation of colorectal cancer. Mod Pathol 32:1-15, 2019 (suppl 1)
49. Indraccolo S, Lombardi G, Fassan M, et al: Genetic, epigenetic, and immunologic profiling of MMR-deficient relapsed glioblastoma. Clin Cancer Res 25:1828-1837, 2019
50. Touat M, Li YY, Boynton AN, et al: Mechanisms and therapeutic implications of hypermutation in gliomas. Nature 580:517-523, 2020
51. Lu M, Zhang P, Zhang Y, et al: Efficacy, safety, and biomarkers of toripalimab in patients with recurrent or metastatic neuroendocrine neoplasms: A multiple-center phase Ib trial. Clin Cancer Res 26:2337-2345, 2020
52. Maggio I, Manuzzi L, Lamberti G, et al: Landscape and future perspectives of immunotherapy in neuroendocrine neoplasia. Cancers (Basel) 12:832, 2020
53. Halperin DM, Liu S, Dasari A, et al: A phase II trial of atezolizumab and bevacizumab in patients with advanced, progressive neuroendocrine tumors (NETs). J Clin Oncol 38, 2020 (suppl 4; abstr 619)
54. Yao JC, Strosberg J, Fazio N, et al: Activity & safety of spartalizumab (PDR001) in patients (pts) with advanced neuroendocrine tumors (NET) of pancreatic (Pan), gastrointestinal (GI), or thoracic (T) origin, & gastroenteropancreatic neuroendocrine carcinoma (GEP NEC) who have progressed on prior treatment (Tx). Ann Oncol 29:viii467-viii468, 2018
55. Hypermutated gliomas respond poorly to immunotherapy. Cancer Discov 10:OF5, 2020

APPENDIX

TABLE A1. Summary of Additional VUS Detected Across Serial Molecular Profiling Performed on Tissue and Plasma Specimens Throughout the Clinical Course

		Same Tissue Specimen			Same Tissue Specimen				
Time	**t = –0.2 Months**	**t = 0 (tissue diagnosis)**		**t = 20.3 Months**	**t = 21.0 Months**		**t = 31.1 Months**	**t = 43.2 Months**	**t = 46.0 Months**
Source	Plasma	Tissue (liver)	Tissue (liver)	Plasma	Tissue (liver)	Tissue (liver)	Tissue (liver)	Plasma	Plasma
Specific test	Guardant360[36]	UCSF500[37,a]	STAMP[38]	FoundationACT[39]	UCSF500[37,a]	GPS Cancer (NantHealth)[40]	UCSF500[37]	Guardant360[36]	Guardant360[36]
VUS	BRAF p.G32R CDKN2A p.L30R RB1 p.T5P	EED p.T8S	APC p.S2242G	None	EED p.T8S IGF2R p.A1074T SOS2 p.S384N ZMYM3 p.L85fs	None	ACVR1B p.G511R AJUBA c.1422+1G>A ALK p.S211F ARID1B p.G1191D ASH2L p.P450L AURKB p.A319V AXL p.V564M BCOR p.E1477K BLM c.960-1G>A C11orf30 p.S388N CBL p.A519V CHD4 p.T758I COL1A1 p.A748V CTCF p.S360N CTNNB1 p.T339I CYLD c.2350+5G>A CYLD p.L840F DCC p.R211Q DUSP6 p.S102N EBF1 c.1744+6C>T EPHA5 p.P904L EPHA7 p.A242T ERBB2 p.G1189D ERBB3 p.P502S ERBB4 p.R426K ERCC2 p.S458F ESPL1 p.L363F EWSR1 c.1693+5G>A FAT1 p.T1511I FOXO1 p.A511T FOXO1 p.G396D GLI1 p.T1074I GLI2 p.A387T GLI2 p.G1311E GRIN2A p.E530K IGF2R p.A1074T IGF2R p.S2147N IKZF3 c.-43C>T INPP4B p.V503M KDR p.L1178F KDR p.G1015S KMT2A p.D3595N KMT2D p.P4281L KMT2D p.G1119E KMT2D p.G794E	ALK p.V1004I ALK p.V1039A APC p.G877D APC p.H2526Y APC p.P1101L APC p.S26N AR p.E252K ARID1A p.G1792D ARID1A p.G1890R ARID1A p.P1259S ARID1A p.P287L ARID1A p.P490S ARID1A p.P517L ARID1A p.Q2207* ATM p.A2451V ATM p.E390K ATM p.G873E ATM p.L1910F ATM p.L2005del ATM p.P1922L ATM p.T547I BRAF p.A497T BRCA1 p.D1546N BRCA1 p.G928D BRCA1 p.S681N BRCA1 p.S945N BRCA2 p.D364N BRCA2 p.P3054S BRCA2 p.P3129S BRCA2 p.R1131K CCND2 p.T93A CCNE1 p.A236T CDK12 p.E674K CDK12 p.P1266L CDK12 p.P326L CDKN2A p.A39T ERBB2 p.E744K FBXW7 p.V424I FGFR1 p.V740M FGFR2 p.D602N GATA3 p.G361S GNA11 splice site SNV GNAS p.V202I HNF1A p.R201K IDH1 p.G105D	APC p.E2719K AR p.E252K ARID1A p.A2167T ARID1A p.P287L ARID1A p.P517L ARID1A p.Q2209* ATM p.G873E ATM p.P1922L BRCA1 p.E1214K BRCA1 p.S681N BRCA2 p.P3129S BRCA2 p.S1538P BRCA2 p.T2783I CCND2 p.T93A CDK12 p.E674K CDK12 p.P326L CDK4 p.S36N CDK6 p.P74S CDKN2A p.A39T ERBB2 splice site SNV ESR1 p.P336S FGFR1 p.T509I FGFR1 p.V740M FGFR2 p.D136N FGFR3 p.S781N IDH1 p.G105D JAK2 p.G614E KIT p.T389I KRAS splice site SNV MAPK3 p.H197N MPL p.G509S MTOR p.G95R MTOR p.Q973* MYC p.G289D NOTCH1 p.R1622C NTRK1 p.C345R PDGFRA splice site SNV ROS1 p.G212D ROS1 p.S1765N STK11 p.A417T TERT promoter SNV TERT splice site SNV TP53 p.G199R TP53 p.R209K

(Continued on following page)

TABLE A1. Summary of Additional VUS Detected Across Serial Molecular Profiling Performed on Tissue and Plasma Specimens Throughout the Clinical Course (Continued)

Time	t = –0.2 Months	Same Tissue Specimen: t = 0 (tissue diagnosis)	t = 20.3 Months	Same Tissue Specimen: t = 21.0 Months	t = 31.1 Months	t = 43.2 Months	t = 46.0 Months
					LRP1B p.L764P	KIT p.D851N	
					LZTR1 c.1449+1G>A	KIT p.S959F	
					MAP3K9 p.E833K	KIT p.V950fs	
					NCOA2 p.A971V	KRAS splice site SNV	
					NCOA3 p.P656S	MAP2K1 p.S140N	
					NCOR1 p.E1987K	MAPK3 p.H197N	
					NF1 p.A761T	MET p.P239L	
					NIPBL c.771+4T>C	MPL p.G509S	
					NOTCH3 p.G172D	MPL p.P518S	
					NUTM1 c.-195C>T	MTOR p.A699T	
					PALB2 p.G257S	MTOR p.G95R	
					PAX8 p.S193N	MTOR p.Q973*	
					PAX8 p.L142F	MTOR p.V936I	
					PBRM1 c.1541+1G>A	MYC p.G289D	
					PDGFRA p.S947N	MYC p.V7M	
					POLQ p.T966I	NOTCH1 p.G2299D	
					PRDM1 p.Y410C	NOTCH1 p.T194I	
					PTCH1 p.S900N	NOTCH1 p.V1648M	
					PTPRB p.R2185K	NTRK1 p.C345R	
					PTPRB p.D976N	PDGFRA splice site SNV	
					SF3B1 p.S956F	PTEN p.E299K	
					SMARCA2 p.V1426I	RAF1 p.L570F	
					SMARCA4 p.D1670N	ROS1 p.G2121D	
					SOS2 p.E968K	ROS1 p.L1937F	
					SOS2 p.S384N	STK11 p.G171D	
					SPEN p.A205T	TERT p.A689V	
					SPTA1 p.E1983K	TERT splice site SNV	
					SPTA1 p.A1523V	TP53 p.A353V	
					SPTA1 p.S1296N	TP53 p.A78T	
					SYNE1 c.22495-6T>A	TP53 p.R209K	
					SYNE1 p.A5712V		
					TET2 p.A457T		
					TET2 p.S972F		
					TLR4 p.A118T		
					TOP2A p.R450*		
					WRN p.G1207D		
					ZFHX4 p.P2469S		
					ZNF217 p.P259S		

Abbreviation: VUS, variants of uncertain significance.

[a]Indicates results that were collected as part of research analysis, which were not available at the time of clinical decision making.